Nanoscale Advances

ROYAL SOCIETY OF CHEMISTRY

PAPER

View Article Online
View Journal | View Issue

Cite this: *Nanoscale Adv.*, 2025, **7**, 1603

Revolutionizing green catalysis: a novel amla seed derived biochar modified g-$C_3N_4 \cdot SO_3H$ catalyst for sustainable and versatile synthesis of bis-indoles†

Shivani Soni, Sunita Teli, Pankaj Teli and Shikha Agarwal *

Catalysis plays a vital role in green chemistry by improving process efficiency, reducing waste, and minimizing environmental impact. A biochar-modified g-$C_3N_4 \cdot SO_3H$ (BCNSA) catalyst was developed using biochar derived from amla seed powder and CNSA. CNSA was synthesized *via* the reaction of g-C_3N_4 with chlorosulfonic acid. Both components were combined, pyrolyzed, purified, and comprehensively characterized using FTIR, XRD, FE-SEM, EDX, elemental mapping, TGA, and DTA studies to confirm the successful synthesis and structural integrity. The catalyst demonstrated exceptional efficiency in synthesizing bis-indole derivatives through reactions between substituted indoles (indole, 1-methyl indole, and 6-chloro indole) and carbonyl-containing compounds, including isatins (isatin, 7-(trifluoromethyl)isatin, 5-bromo isatin, and 5-fluoro isatin), aldehydes, cyclo-ketones, dimedone, and acetophenones. These reactions were carried out under simplified conditions using water as a green solvent, promoting sustainability and versatility. A total of 21 bis-indole products were synthesized within 5–45 minutes, achieving yields of 80–98% showcasing the catalyst's outstanding performance. Furthermore, the method was scaled up to gram-level synthesis, and green chemistry metrics were evaluated for all the products, highlighting the environmental and economic benefits of this approach.

Received 28th October 2024
Accepted 10th January 2025

DOI: 10.1039/d4na00891j

rsc.li/nanoscale-advances

Introduction

Heterocyclic compounds, which feature ring structures containing heteroatoms such as nitrogen, oxygen, or sulfur, are pivotal in chemistry owing to their wide range of applications in pharmaceuticals, natural products, and materials science.[1] Indoles and bis-indoles stand out due to their chemical versatility and significant biological activities.[2] Indoles, with a benzene ring fused to a pyrrole ring, exhibit reactive sites at the C3 position, allowing various functionalizations.[3] They are moderately polar, slightly soluble in water, and highly soluble in organic solvents, displaying good stability under mild conditions.[4] Bis-indoles, comprising two linked indole units, have increased molecular complexity, leading to higher melting points and lower water solubility.[3] These characteristics enhance their wide spectrum of biological activities, including anticancer,[5] antiviral,[6] antimicrobial,[5] antioxidant,[5] anti-inflammatory,[5] antifungal,[7] and spermicidal[7] effects, making them crucial in drug development and sustainable synthesis (Fig. 1). However, synthesizing bis-indoles is challenging due to difficulties in selectively coupling indole units, often resulting in side reactions and low yields. Traditional methods are often inefficient, involving multiple steps and complex reaction conditions, highlighting the need for more efficient and sustainable approaches. Recently, bis-indole derivatives were synthesized by Adly *et al.*[8] using deep eutectic solvents (DESs), while Chavan and coworkers[9] employed taurine as a catalyst. Although these methods are effective, their major limitation lies in the narrow substrate scope, which restricts their applicability to a broader range of indole derivatives. To overcome this limitation, we have developed a more versatile catalytic approach with improved substrate compatibility and efficiency.

In this context, catalysis plays a vital role in green chemistry by improving process efficiency, reducing waste, and minimizing environmental impact.[10] Catalysts enable milder reaction conditions and better selectivity, promoting eco-friendly chemical synthesis.[10] Conventional catalysts face limitations such as limited reusability, deactivation under harsh conditions, and contamination, necessitating the development of more sustainable alternatives.[11] Graphitic carbon nitride (g-C_3N_4) emerges as a versatile catalyst exhibiting high thermal stability and semiconductor properties. It is used effectively in photocatalysis for pollutant degradation and hydrogen production, as well as in organic reactions such as oxidation and cross-coupling.[12] Acid modification of g-C_3N_4 enhances its catalytic performance by introducing functional groups that improve acidity and surface interactions, making it more effective for specific applications.[12] Similarly, biochar (BC)

Synthetic Organic Chemistry Laboratory, Department of Chemistry, MLSU, Udaipur-313001, Rajasthan, India. E-mail: shikhaagarwal@mlsu.ac.in; shivanisoni8811@gmail.com

† Electronic supplementary information (ESI) available. See DOI: https://doi.org/10.1039/d4na00891j

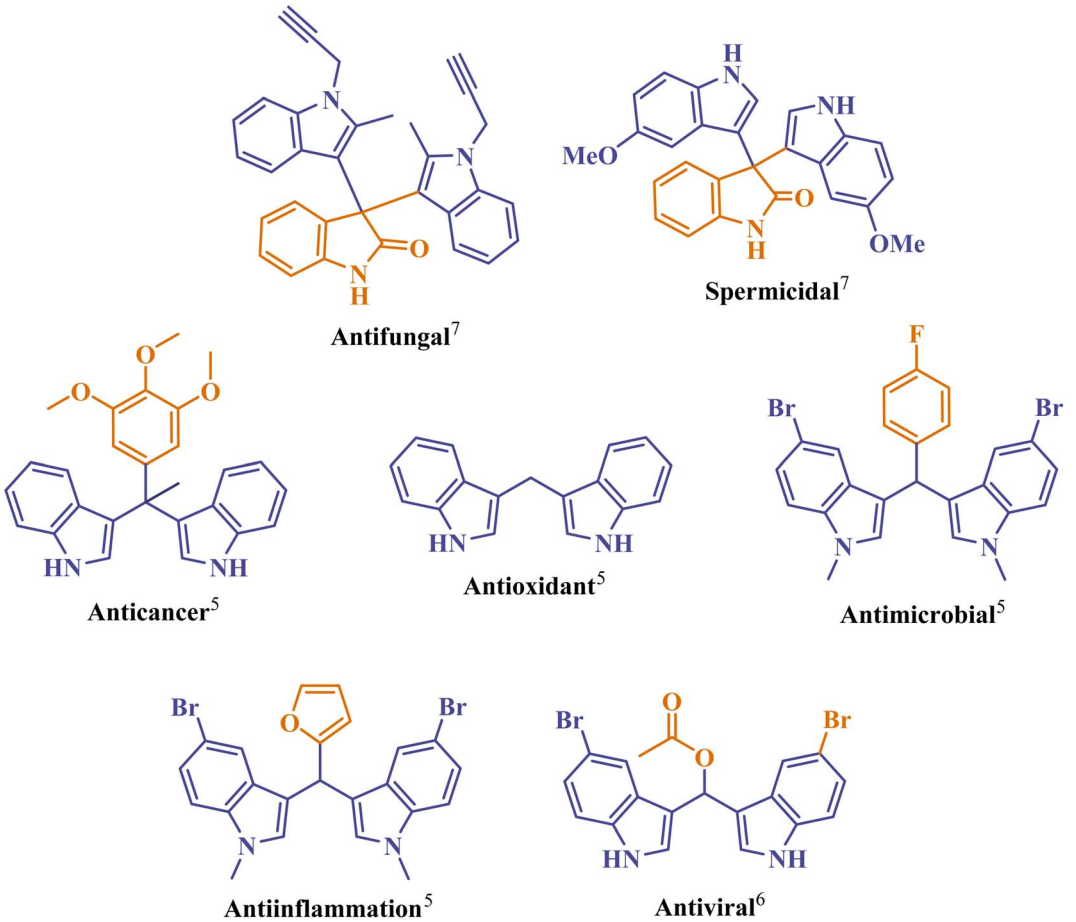

Fig. 1 Biologically active bis-indole derivatives.

modifications enhance the catalytic activity of materials by increasing surface area, stability, and porosity, improving performance and durability.[13] Derived from waste biomass, biochar is a sustainable and cost-effective option that supports environmentally friendly practices while offering efficient solutions for various catalytic applications.[13]

Keeping in mind the robust properties of g-C_3N_4 and biochar, we have developed a groundbreaking novel biochar-modified g-C_3N_4·SO_3H (BCNSA) catalyst, meticulously characterized by FTIR, XRD, FE-SEM, EDX, mapping, TGA, and DTA analyses to ensure its successful synthesis and structural integrity. This advanced catalyst demonstrates exceptional efficiency in facilitating the synthesis of a diverse range of bis-indoles, catalyzing reactions between indoles and carbonyl groups containing reactants such as isatins, aldehydes, cycloketones, and acetophenones. By adopting simplified reaction conditions and utilizing water as the solvent, our approach not only fosters a more sustainable and environmentally friendly process but also offers superior efficiency and versatility in organic synthesis. This innovative catalyst represents a significant advancement in sustainable chemical processes, enhancing both the economic and environmental aspects of bis-indole synthesis.

Results and discussion

The synthesis of the BCNSA catalyst was conducted by treating amla seed derived BC with CNSA and characterized through a variety of analytical techniques, including FT-IR, XRD, SEM, EDX, mapping, TGA, and DTA analyses. FT-IR spectra were recorded for urea, g-C_3N_4 (CN), g-C_3N_4·SO_3H (CNSA), amla seed powder (ASP), biochar (BC), and BC@g-C_3N_4·SO_3H (BCNSA) across a 500–4000 cm^{-1} range to examine the observed variations, as depicted in Table 1,[14,15] (Fig. 2).

The XRD analysis of the BCNSA catalyst revealed notable structural modifications. CNSA initially showed peaks at 13.12° (100 plane) and 27.84° (002 plane), while biochar has a peak at

Table 1 Some signature IR absorption peaks of CNSA, BC, and BCNSA

S. n.	Bond	CNSA (cm^{-1})	BC (cm^{-1})	BCNSA (cm^{-1})
1	O–H	3350–3500	3700	3400–3700
2	N–H	3000–3350	3000	3028–3177
3	CH_2	2823–2880	2800–2831	2800
4	C–N, C=N	1200–1600	1400	1160–1285
5	C–N–S	800	—	840
6	C=C	1500–1630	1600	1584
7	S=O	640	—	670

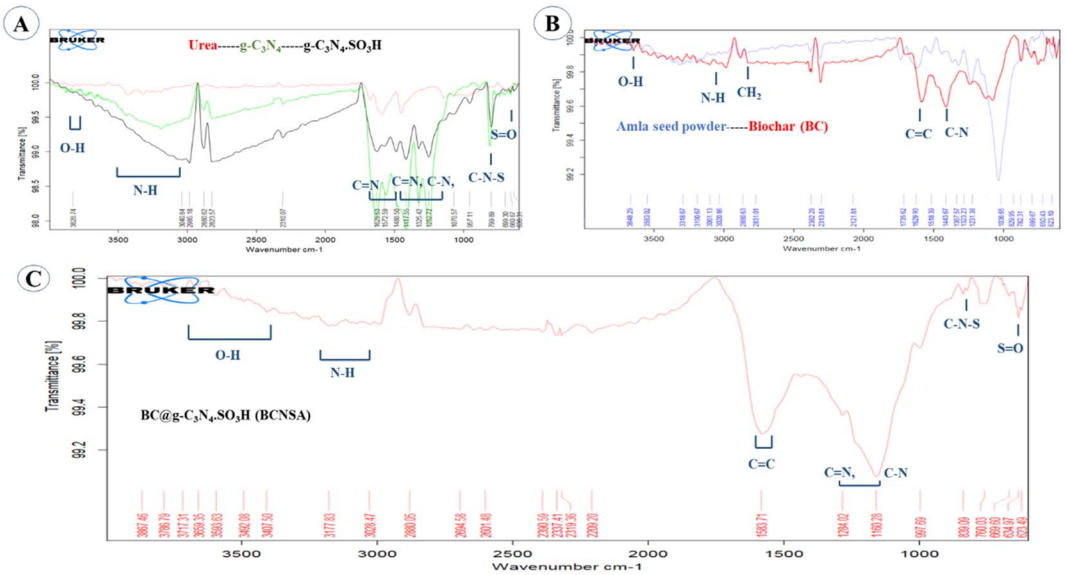

Fig. 2 The comparison FT-IR spectra of (A) CNSA, (B) BC, and (C) BCNSA catalyst.

24.16° (002 plane). For the BCNSA catalyst, the 100-plane peak at 13.12° disappeared, suggesting a disruption in the CN's in-plane structural order. The peak at 25.44° (002 plane) indicated that the biochar structure remains present, but the shift from 27.84° to 25.44° suggested an alteration in CN's interlayer spacing due to interaction with biochar. Additionally, the new peak at 42.79° implies the formation of a new crystalline phase, potentially resulting from the incorporation of SO_3H groups or other changes during the reaction, leading to a hybridized structure[14,16] (Fig. 3).

The FESEM images of BCNSA, displayed in Fig. 4, revealed a graphite-like structure characterized by distinct layers, rough textures, and a porous surface morphology. The EDX spectra, presented in Fig. 5(A–C), further support these observations, while the elemental mapping in Fig. 5(D–H) illustrates the distribution of individual elements (C, N, S, and O). The results confirmed the expected elemental composition and demonstrated the uniform dispersion of C, N, S, and O, especially from the functionalized sulfonic acid groups, reinforcing the successful modification of the catalyst.[16,17]

The TGA data for the BCNSA catalyst indicated good thermal stability. A 15.2% weight loss from RT to 150 °C suggests the evaporation of adsorbed moisture or volatile compounds. From 150 °C to 1000 °C, an additional 27.4% was decomposed, with

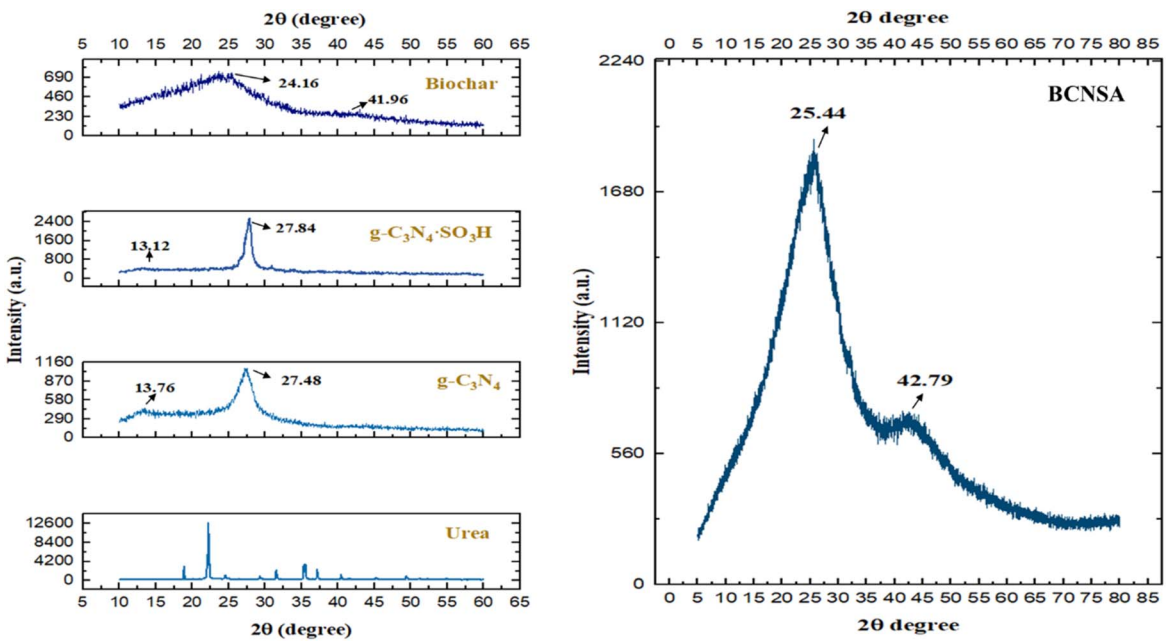

Fig. 3 The XRD graph of urea, g-C_3N_4, g-C_3N_4·SO_3H, biochar and the synthesized BCNSA catalyst.

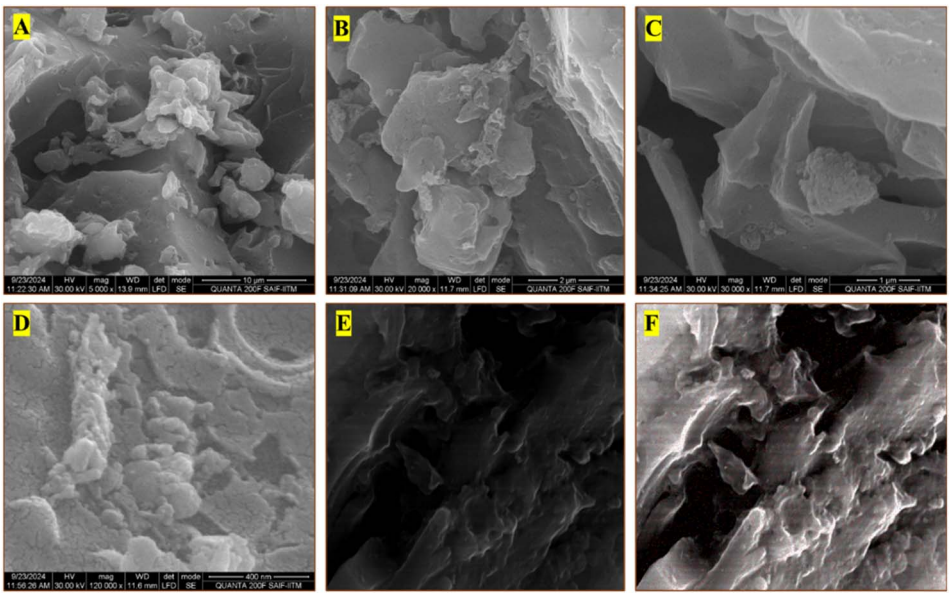

Fig. 4 FESEM images (A–F) of the BCNSA catalyst across different magnifications.

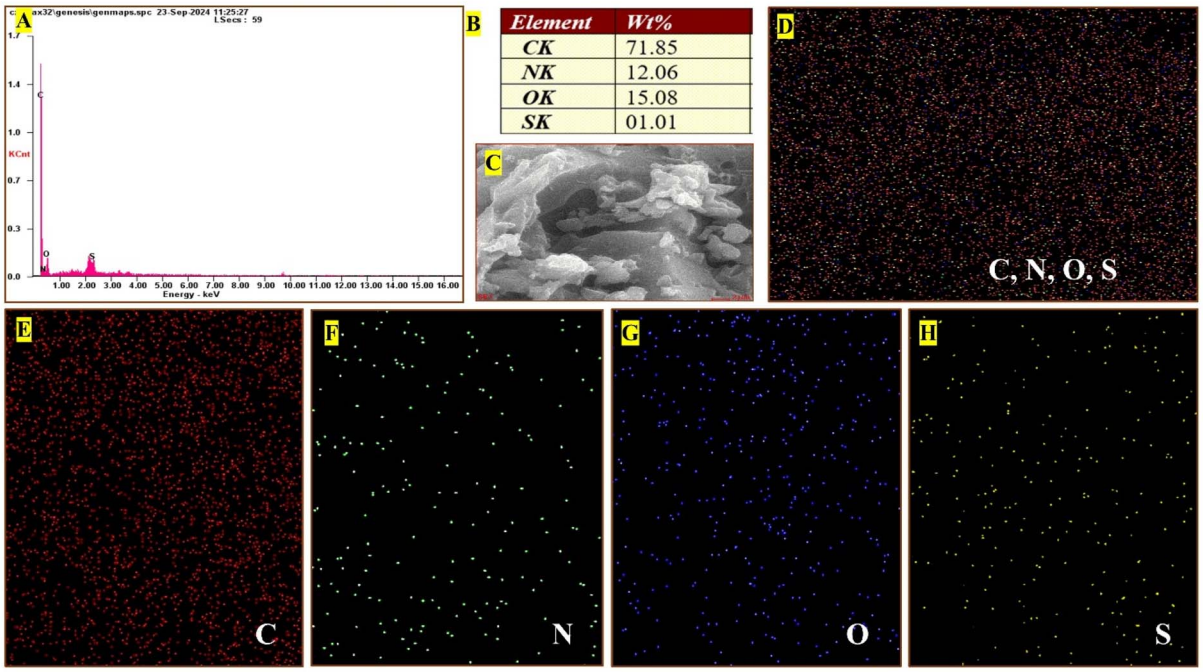

Fig. 5 EDX spectra (A–C) and elemental mapping (D–H) of the BCNSA catalyst.

only 19% loss up to 500 °C. This implies that after the initial volatilization, a slower decomposition occurred between 150 °C and 500 °C, likely involving more stable organic groups or surface functionalities. The remaining decomposition above 500 °C suggests the breakdown of more thermally stable materials, confirming that the catalyst maintains significant structural integrity up to high temperatures (Fig. 6A). The DTA data show three key thermal events. From room temperature to 65 °C, an endothermic process was observed, likely corresponding to the evaporation of moisture or volatiles. Between 65 °C and 510 °C, an exothermic reaction occurred, indicating the decomposition or combustion of organic material. Finally, from 510 °C to 1000 °C, the exothermic activity decreased, signaling the completion of decomposition and the development of a more stable residue. This indicates that the material experienced moisture loss and decomposition (42.6%) at high temperatures up to 1000 °C, demonstrating the catalyst's high thermal stability (Fig. 6B).

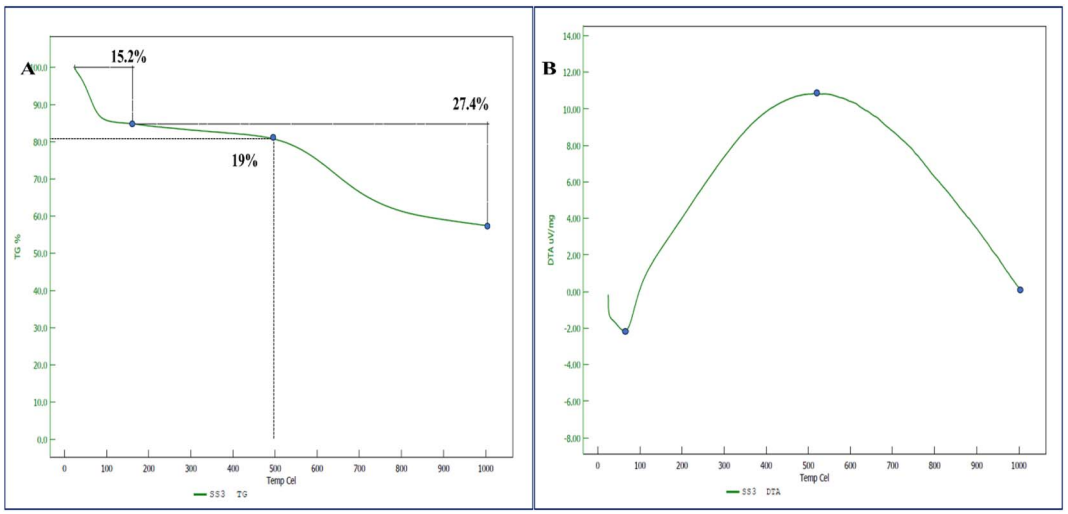

Fig. 6 The (A) TGA and (B) DTA graphs of the synthesized BCNSA catalyst.

To achieve an efficient and eco-friendly synthesis of bis-indoles, we embarked on a systematic optimization process [Table 2]. Using 1-methyl indole (0.5 mmol) (**1a**) and 7-(trifluoromethyl)isatin (0.25 mmol) (**2a**) as model reactants, we aimed to synthesize 1,1″-dimethyl-7′-(trifluoromethyl)-1*H*,1″*H*-[3,3′:3′,3″-terindol]-2′(1′*H*)-one (**5A**). A comprehensive evaluation of reaction conditions was conducted, beginning with the catalyst and solvent-free trials, followed by the utilization of

Table 2 Optimization of reaction conditions with 7-CF_3-isatin influenced bis-indole derivatives

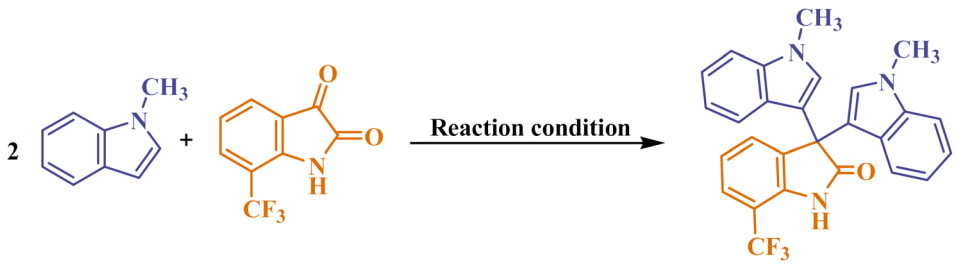

1a **2a** **5A**

S. n.	Catalyst	Catalyst loading	Solvent	Temperature	Time	Yield (%)
1	—	—	—	RT	>48 h	—
2	—	—	H_2O	RT	>48 h	—
3	Acetic acid	25 mg	H_2O	RT	20 h	35
4	Chitosan-SO_3H	25 mg	H_2O	RT	1 h	68
5	Urea	25 mg	H_2O	RT	6 h	53
6	g-C_3N_4	25 mg	H_2O	RT	5 h	57
7	g-C_3N_4·SO_3H	25 mg	H_2O	RT	30 min	78.48
8	g-C_3N_4·SO_3H	25 mg	H_2O	Reflux	30 min	78.27
9	g-C_3N_4·OH	25 mg	H_2O	RT	30 min	73.54
10	g-C_3N_4·OH	25 mg	H_2O	Reflux	30 min	71.24
11	BC@SO_3H	25 mg	H_2O	RT	30 min	67.37
12	BC@SO_3H	25 mg	H_2O	Reflux	30 min	66.43
13	BCNSA	25 mg	H_2O	RT	5 min	84.93
14	BCNSA	30 mg	H_2O	RT	5 min	85.19
15	**BCNSA**	**20 mg**	**H_2O**	**RT**	**5 min**	**85.47**
16	BCNSA	20 mg	H_2O	Reflux	5 min	85.41
17	BCNSA	15 mg	H_2O	RT	10 min	84.11
18	BCNSA	10 mg	H_2O	RT	10 min	80.01
19	BCNSA	20 mg	H_2O + EtOH	RT	5 min	83.23
20	BCNSA	20 mg	EtOH	RT	5 min	78.76
21	BCNSA	20 mg	Ultrasound	RT	30 min	81.57
22	BCNSA	20 mg	Blue light	RT	40 min	79.64

water as a solvent. Despite 48 hours of reaction time, no product formation was observed [Table 2; entries 1 and 2]. We then turned to a range of catalysts available in our research laboratory. While product formation was achieved, the yields were inconsistent across different catalysts [Table 2; entries 3–10], with entry 7 yielding the most promising result. However, we remained unsatisfied, as our goal was to identify the most efficient and sustainable method. This led us to synthesize BCSA (BC@SO_3H), but the results were suboptimal [Table 2; entries 11 and 12]. Undeterred, we synthesized BCNSA, which delivered significantly improved outcomes. We proceeded to optimize the parameters of the reaction with BCNSA, exploring catalyst loading, solvent variation, and temperature adjustments. Additionally, we introduced sonication and blue light activation to further enhance the reaction [Table 2; entries 13–22]. Ultimately, Table 2; entry 15 emerged as the optimal condition, employing 20 mg of catalyst in water at room temperature, marking a significant breakthrough in our quest for a green and efficient synthetic route.

After optimizing the reaction conditions, we successfully synthesized a diverse array of bis-indole derivatives. To expand the scope, we varied the indole reactants (*e.g.*, indole, 1-methyl indole, and 6-chloro indole) and explored different isatins (*e.g.*, isatin, 7-(trifluoromethyl)isatin, 5-bromo isatin, and 5-fluoro isatin) [Scheme 1(a)]. Furthermore, we introduced a variety of aldehydes, cyclo-ketones, acetophenones, and dimedone to achieve broad functionalization and structural diversity in bis-indole derivatives. The optimized conditions proved to be highly effective for reactions with aldehydes and acetophenones, resulting in high yields and purity [Scheme 1(b)]. However, reactions with cyclo-ketones and dimedone initially showed limited success at room temperature. By shifting to reflux conditions, the reactions significantly improved, yielding products in satisfactory amounts [Scheme 1(c)].

This adjustment not only expanded the versatility of our method but also demonstrated its applicability to a broader range of substrates, making it a robust and adaptable approach for synthesizing bis-indole derivatives. Fig. 7 provides the complete library of synthesized compounds. Table 3 summarizes previously reported techniques for synthesizing bis-indole derivatives, highlighting their diversity and providing a comparison with our work. In the suggested mechanism (Scheme 2) for synthesizing bis-indoles,[25,26] it is presumed that the BCNSA catalyst initially formed a hydrogen bond with the carbonyl oxygen atom and activated it. This activated species was believed to undergo a Knoevenagel condensation with indole, causing the formation of intermediate **I** after the elimination of a water molecule. Intermediate **I** was then presumed to react with a second indole molecule *via* Michael addition, yielding intermediate **II**. Following tautomerization, intermediate **II** was believed to convert into the final bis-indole product [**III**].

The differences in reaction time and yield can be attributed to the distinct electronic and steric effects of the aldehyde substituents. Electron-withdrawing groups (EWGs) enhance the electrophilicity of the carbonyl carbon, making it more reactive towards nucleophilic attack. For example, the thiazole ring in **5M** stabilized the transition state, and the methyl group introduced minimal steric hindrance, leading to a faster reaction and higher yield. On the other hand, electron-donating groups (EDGs), such as the methoxy groups in **5Q**, decreased the electrophilicity of the aldehyde carbonyl, slowing the reaction and

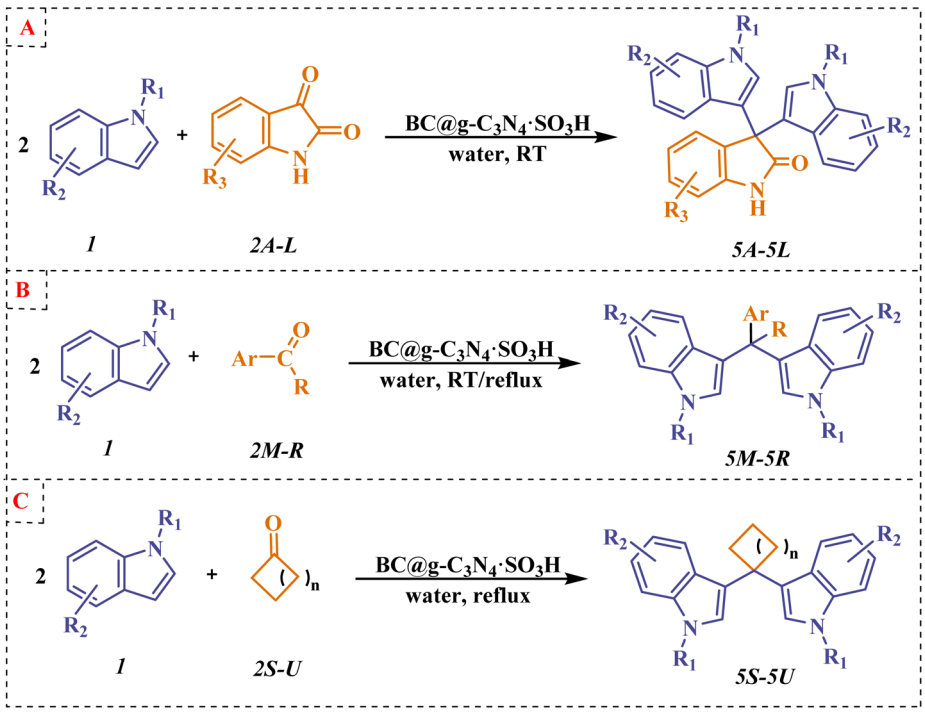

Scheme 1 Synthetic pathways to bis-indole derivatives.

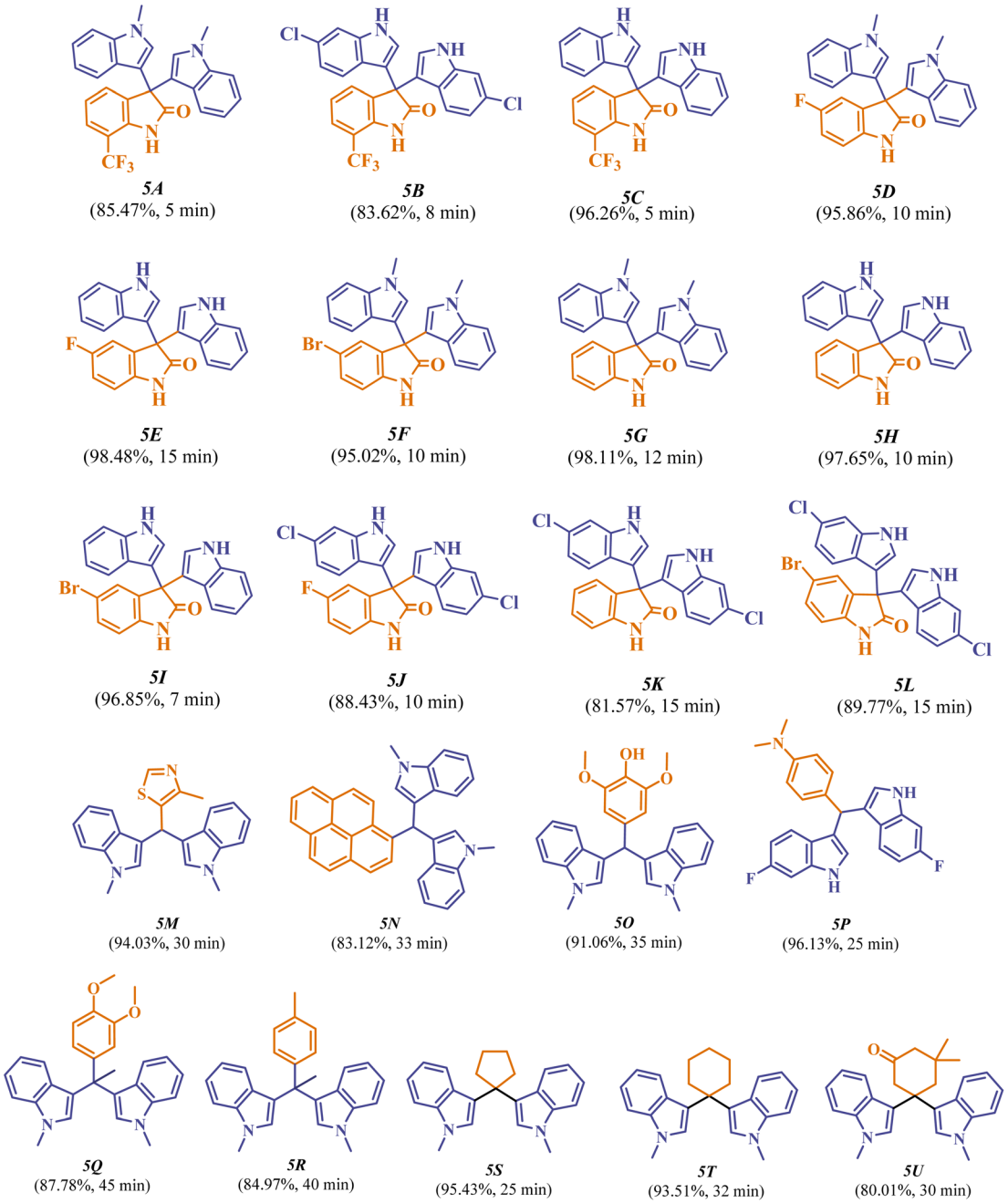

Fig. 7 Library of synthesized bis-indole scaffolds (compounds 5A–5R; in water at RT. Compounds 5S–5U; in water at reflux).

Table 3 Reported synthetic approaches for preparing a bis-indole (5H) derivative with the present work

S. n.	Catalyst	Reaction conditions	Time	Yield (%)	Ref.
1	Sulfamic acid (20 mol%)	EtOH : H_2O (1 : 1), RT	2 h	89	18
2	Molecular iodine (5 mol%)	Isopropanol	15 min	98	19
3	SiO_2-OSO_3H (0.2 g)	CH_2Cl_2, RT	2 h	94	20
4	Thiamine hydrochloride (1 mol%)	Solvent-free, RT	1 h	90	21
5	Br_2 (3 mol%)	CH_3CN, reflux	4 h	95	22
6	β-CD-SO_3H (10 mol%)	H_2O, reflux	10 min	95	23
7	Amberlyst 15 (0.3 g)	H_2O, 70 °C	30 min	94	24
8	BC@g-C_3N_4·SO_3H (20 mg)	Water, RT	10 min	97.65	This work

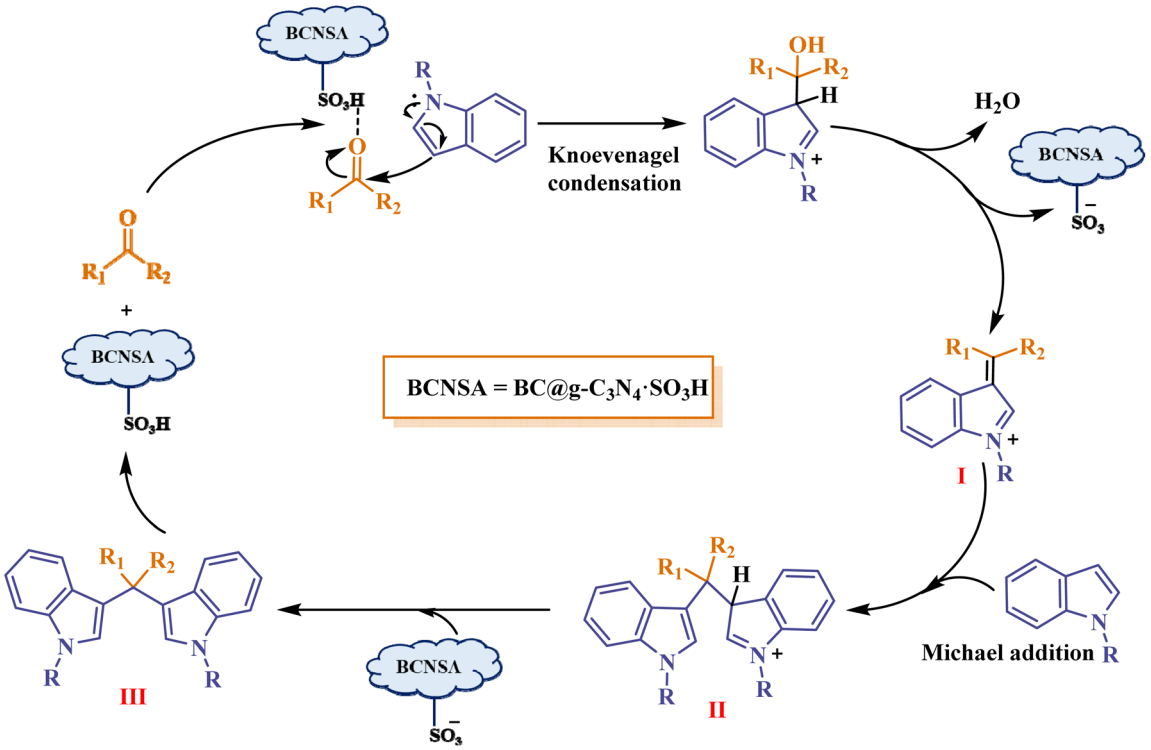

Scheme 2 The proposed reaction mechanism for synthesizing bis-indole scaffolds.

lowering the yield. Additionally, steric effects play a crucial role in the reaction efficiency. Despite the electron-withdrawing aldehyde group in **5N**, the bulky pyrene ring introduced significant steric hindrance, preventing efficient nucleophilic attack and thereby reducing both the reaction rate and the yield.

Catalyst reusability

The catalyst was recycled by first removing it from the reaction mixture using methanol, as the synthesized compound was soluble in it. The catalyst was then filtered, washed several times with acetone to remove impurities, and dried before reuse. Following the successful synthesis of bis-indole scaffolds, we evaluated the reusability of the BCNSA catalyst using **5I** as the model reaction. The catalyst was recycled across six successive cycles. During the first four cycles, the yields remained consistent with no noticeable loss in efficiency. After the sixth cycle, a slight color change from black to faded black was observed, accompanied by a 5% reduction in the yield. However up to the sixth cycle, the recovered catalyst amount was substantial, despite a slight weight loss, and product yields remained high. Also, after the sixth cycle, an additional 2 mg loss was observed, totaling a 7 mg reduction from the initial catalyst weight by the seventh cycle. This study confirmed that the BCNSA catalyst can be effectively recycled and reused up to 6 times with negligible loss in the activity, demonstrating both its efficiency and sustainability over repeated use (Fig. 8). The FTIR spectrum of the reused catalyst after the 6th cycle is almost identical to that of the fresh catalyst, indicating that the catalyst's structure remains intact and has not been distorted even after six cycles of reuse (Fig. 9).

Hot filtration test

To confirm the heterogeneity of the BCNSA catalyst during the synthesis of bis-indole derivatives, a hot filtration test was performed as follows:

The reaction was conducted by stirring indole (2 mmol) and isatin (1 mmol) in water at RT in the presence of the BCNSA catalyst (20 mg). The reaction mixture was allowed to proceed for 5 minutes, at which point both the product and reactants were present in detectable amounts, as confirmed by TLC analysis. At the 5-minute mark, the reaction mixture was rapidly filtered to remove the solid BCNSA catalyst. The filtration was carried out using a pre-heated filter system to ensure that the reaction mixture remained at the reaction temperature and to avoid any precipitation of potentially dissolved catalytic species. The clear filtrate, now free of the BCNSA catalyst, was transferred to a clean reaction vessel and stirred under identical reaction conditions for an extended period. Samples were periodically collected and analyzed using TLC to monitor the reactants' consumption and the product's formation. Despite stirring for 1 hour, the reaction showed minimal progress, whereas the same reaction reached completion within 10 minutes in the presence of the catalyst. These observations confirmed that the BCNSA catalyst is heterogeneous, with no significant leaching of active species into the reaction medium.

Gram scale synthesis

We evaluated this methodology for its potential industrial application by performing a gram-scale synthesis using 1-methylindole and 7-(trifluoromethyl)isatin (for **5A**) at room

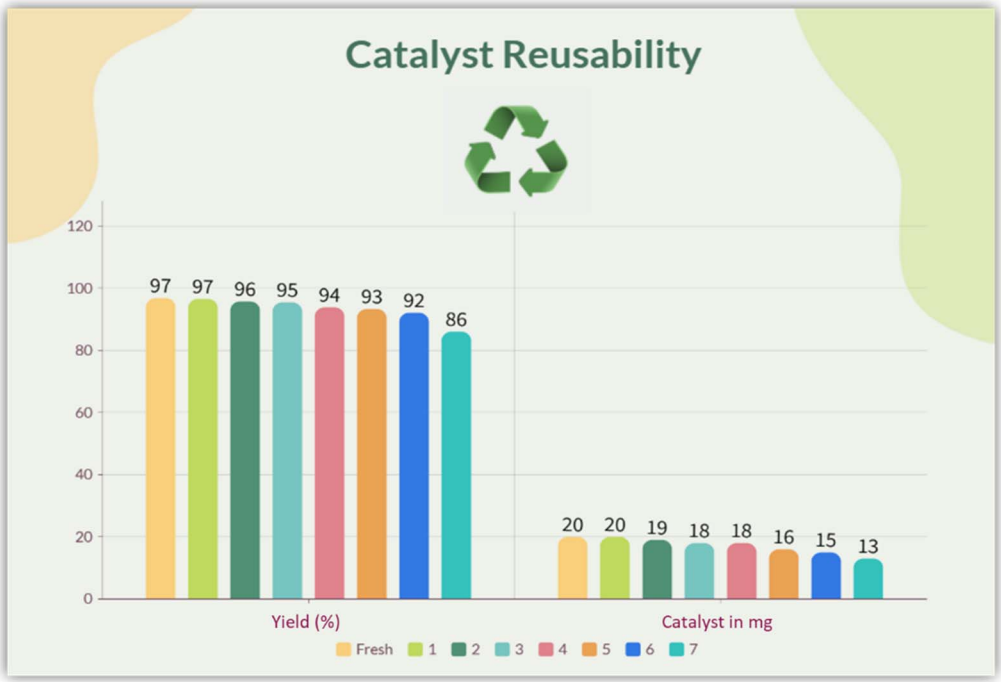

Fig. 8 Reusability study of the BCNSA catalyst.

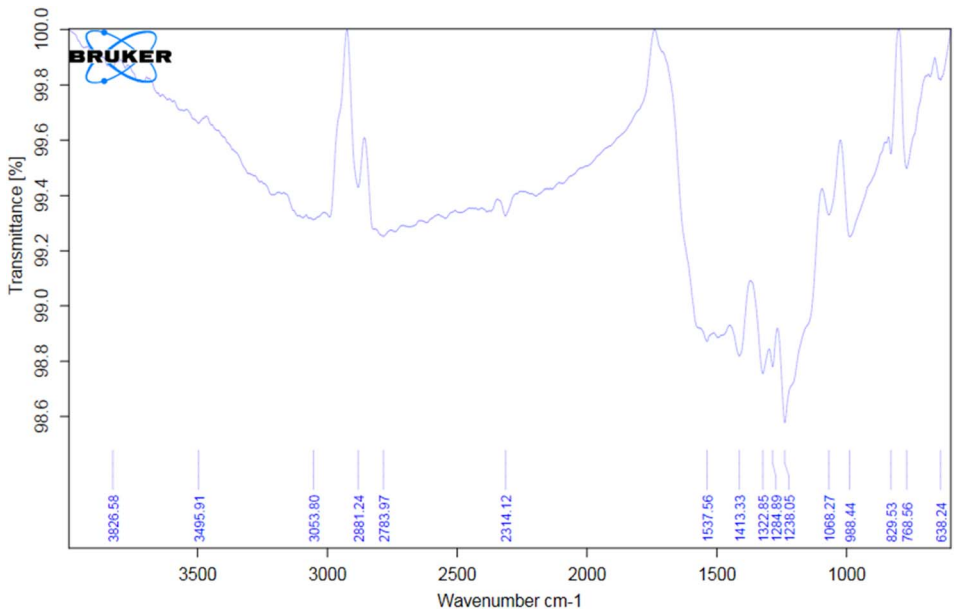

Fig. 9 FT-IR spectrum of the reused BCNSA catalyst after the 6th cycle.

temperature with 20 mg of catalyst, using water as the sole solvent. The reaction was completed in just 35 minutes, as observed by TLC. Notably, after the reaction completion, the mixture underwent a distinct color change to hot pink. This color shift is characteristic of the process, though the specific hue may vary depending on the reactants involved. After the reaction, the reaction mixture was initially dried and then dissolved in methanol. The catalyst was filtered out and subsequently washed with acetone solvent. The filtrate was dried, rinsed with lukewarm water, and dried again. The yield was calculated to be 81.97% (Scheme 3).

Green chemistry metrics

In recent years, there has been a significant shift toward the development of eco-friendly and green methods for synthesizing organic compounds.[27,28] Green chemistry has emerged as a key approach, offering a comprehensive structure for

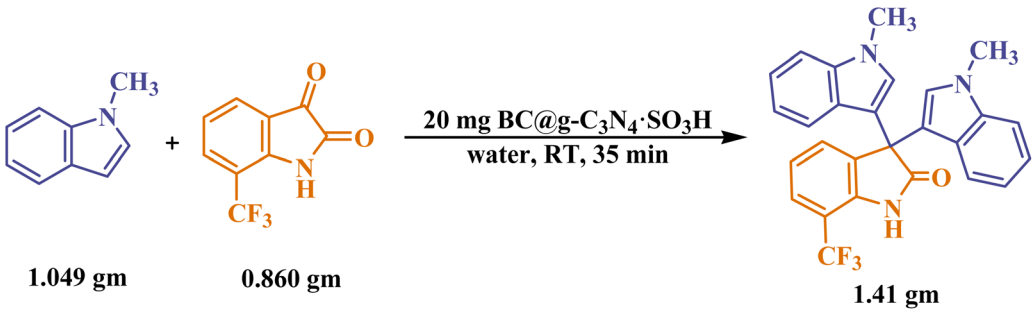

Scheme 3 The scale-up synthesis of 7-CF_3-isatin and indole-derived bis-indole.

evaluating the environmental impact of chemical processes. A prime example is using BCNSA as a catalyst in synthesizing bis-indole derivatives. This method demonstrates outstanding green metrics, including a low *E*-factor (0.064–0.30), high atom economy (94.78–96.30%), excellent reaction mass efficiency (76.41–93.97%), and superior process mass intensity (1.07–1.32). Furthermore, the eco-score (70–79.24) highlights its minimal environmental footprint. These findings underscore the potential of BCNSA catalysts in advancing sustainable, eco-friendly synthesis, offering an efficient approach with minimal ecological impact.

Experimental section

Synthesis of BCNSA

The synthesis of the BCNSA catalyst involved three stages: (a) preparation of BC, (b) synthesis of CNSA, and finally (c) formation of BCNSA (Fig. 10).

Synthesis of BC. Amla seeds were initially sun-dried and then further dried in an oven at 100 °C to ensure complete dehydration. Once fully dried, the seeds were finely ground into powder and sieved. 10 g of the sieved amla seed powder was placed in a crucible, sealed with a lid, wrapped in aluminum foil, and pyrolyzed at 400 °C for 3 hours in a muffle furnace. This resulted in the production of 0.998 g of biochar.

Synthesis of CNSA. g-C_3N_4·SO_3H (CNSA) was synthesized using a previously established method.[15] The procedure involved the dropwise addition of 5 mL chloro-sulfonic acid to 1 g of g-C_3N_4, maintaining the temperature between 0 and 5 °C while stirring continuously for 6 hours. Afterward, the mixture was washed with an ethanol–water solution and later with water to ensure the complete removal of unreacted acid and impurities. The final product was collected in ethanol and dried at 60 °C for 12 hours, resulting in 0.97 g of light yellow CNSA.

Synthesis of BCNSA. The synthesized BC and CNSA were ground together and transferred to a crucible for pyrolysis at

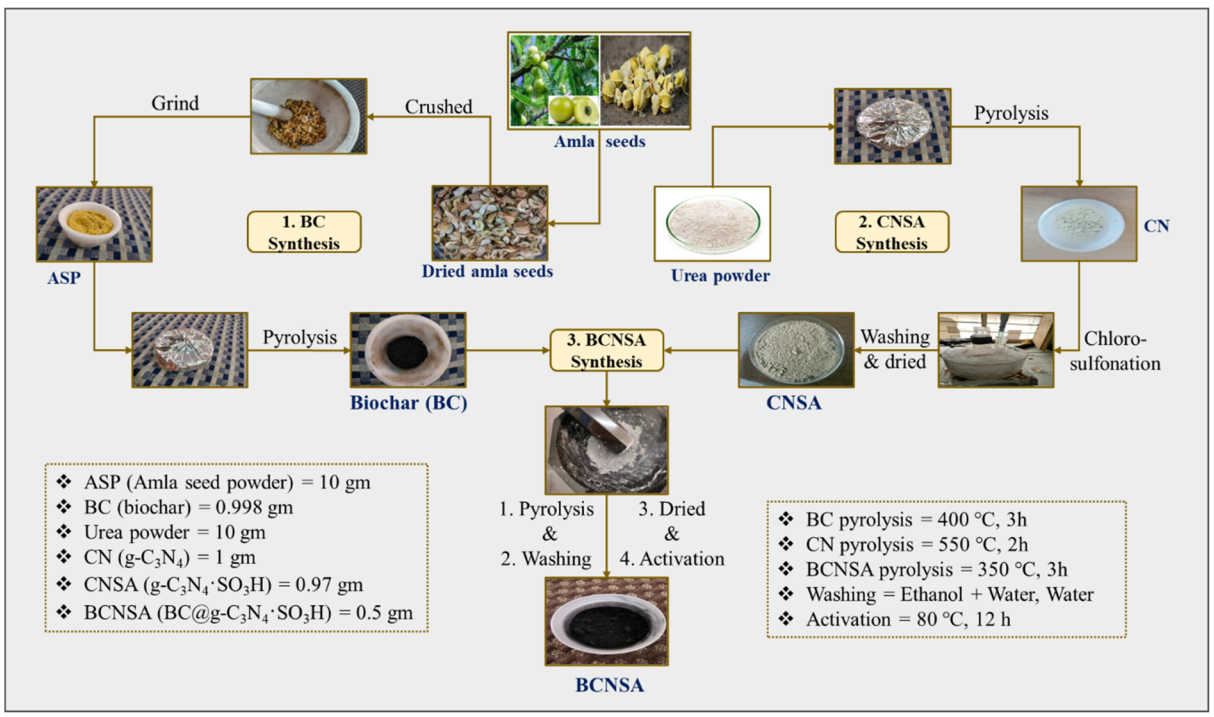

Fig. 10 Step by step pictorial representation for the development of the BCNSA catalyst.

350 °C for 3 hours in a muffle furnace, to yield a black solid. The product was washed thrice with ethanol and twice with water to remove impurities. It was then dried and activated in an oven at 80 °C for 12 hours, yielding 0.5 g of BCNSA.

Synthesis of bis-indole derivatives

In a 25 mL round-bottom flask, 4 mL of water was combined with 0.5 mmol of indole and 0.25 mmol of a second carbonyl group containing reactants such as isatins, aldehydes, acetophenone, cyclo-ketones, or dimedone along with 20 mg of BCNSA catalyst. The mixture was stirred at RT (for **5A–5R**) or under reflux (for **5S–5U**) for an appropriate duration, with the reaction progress monitored by TLC using a 30% solution of ethyl acetate and hexane (30 : 70). During the reaction, the color of the mixture exhibited a notable transformation, shifting from lighter to darker shades, and, in some cases, changing from white to dark red, pink, or orange upon completion. After the reaction, the mixture was dried under vacuum. Then, 10 mL of methanol was added to dissolve the product, leaving the catalyst insoluble. The catalyst was removed by filtration, and any remaining colored residue was further washed with acetone for the complete purification of the catalyst. The filtrate was dried and washed with lukewarm water to remove residual impurities, dried again, and then purified using crystallization. The melting point of the final product was determined, followed by analysis using ^{1}H and ^{13}C NMR spectroscopy to confirm its purity and verify successful synthesis.

NMR and mass spectra of synthesized bis-indole derivatives

5A: 1,1″-Dimethyl-7′-(trifluoromethyl)-1*H*,1″*H*-[3,3′:3′,3″-terindol]-2′(1′*H*)-one. Saffron coloured powder, M. P.: 230–234 °C, ^{1}H NMR (400 MHz, DMSO-d$_6$) δ 11.11 (s, 1H, NH), 7.51 (d, J = 7.9 Hz, 1H, ArH), 7.46 (d, J = 7.3 Hz, 1H, ArH), 7.37 (s, 1H, ArH), 7.35 (s, 1H, ArH), 7.18 (s, 1H, ArH), 7.16 (s, 1H, ArH), 7.10–7.04 (m, 3H, ArH), 6.86 (s, 2H, ArH), 6.84–6.80 (m, 2H, ArH), 3.68 (s, 6H, N-CH$_3$). ^{13}C NMR (101 MHz, DMSO-d$_6$) δ 179.42, 137.92, 136.65, 129.42, 129.14, 126.28, 122.41, 121.78, 121.15, 119.19, 115.46, 112.91, 110.51, 51.99, 32.91. ESI-MS (m/z): 459.1558 [M$^+$] for $C_{27}H_{20}F_3N_3O$.

5B: 6,6″-Dichloro-7′-(trifluoromethyl)-1*H*,1″*H*-[3,3′:3′,3″-terindol]-2′(1′*H*)-one. Brown solid, M. P.: 182–186 °C, ^{1}H NMR (400 MHz, DMSO-d$_6$) δ 11.19 (d, J = 2.2 Hz, 2H, NH), 11.15 (s, 1H, NH), 7.52 (d, J = 8.0 Hz, 1H, ArH), 7.45 (d, J = 7.4 Hz, 1H, ArH), 7.38 (d, J = 1.8 Hz, 2H, ArH), 7.11 (d, J = 8.7 Hz, 3H, ArH), 6.86 (d, J = 2.5 Hz, 2H, ArH), 6.83 (d, J = 1.9 Hz, 1H, ArH), 6.81 (d, J = 1.9 Hz, 1H, ArH). ^{13}C NMR (101 MHz, DMSO-d$_6$) δ 179.25, 137.88, 136.15, 127.82, 126.53, 126.02, 124.71, 122.52, 122.16, 119.51, 114.04, 112.70, 111.92, 111.21, 109.99, 109.78, 51.82. ESI-MS (m/z): 499.0466 [M$^+$], found: 499.0357 for $C_{25}H_{14}Cl_2F_3N_3O$.

5C: 7′-(Trifluoromethyl)-1*H*,1″*H*-[3,3′:3′,3″-terindol]-2′(1′*H*)-one. Beige coloured powder, M. P.: 242–246 °C,[3] ^{1}H NMR (400 MHz, DMSO-d$_6$) δ 11.09 (s, 1H, NH), 11.03 (d, J = 2.1 Hz, 2H, NH), 7.50 (d, J = 8.0 Hz, 1H, ArH), 7.45 (d, J = 7.4 Hz, 1H, ArH), 7.33 (d, J = 8.2 Hz, 2H, ArH), 7.17 (d, J = 8.1 Hz, 2H, ArH), 7.08 (t, J = 7.7 Hz, 1H, ArH), 7.01–6.97 (m, 2H, ArH), 6.82 (d, J = 2.5 Hz, 2H, ArH), 6.81–6.76 (m, 2H, ArH). ^{13}C NMR (101 MHz, DMSO-d$_6$) δ 179.61, 139.13, 137.47, 136.76, 129.44, 125.95, 124.97, 122.96, 122.27, 121.65, 120.98, 119.00, 113.84, 112.30, 111.01, 52.18. ESI-MS (m/z): 431.1245 [M$^+$] for $C_{25}H_{16}F_3N_3O$.

5D: 5′-Fluoro-1,1″-dimethyl-1*H*,1″*H*-[3,3′:3′,3″-terindol]-2′(1′*H*)-one. Beige powder, M. P.: 262–266 °C,[18] ^{1}H NMR (400 MHz, DMSO-d$_6$) δ 10.65 (s, 1H, NH), 7.36 (s, 1H, ArH), 7.34 (s, 1H, ArH), 7.20 (s, 1H, ArH), 7.18 (s, 1H, ArH), 7.07–7.03 (m, 3H, ArH), 7.02–6.98 (m, 1H, ArH), 6.94 (dd, J = 8.4, 4.5 Hz, 1H, ArH), 6.90 (s, 2H, ArH), 6.81 (ddd, J = 8.0, 7.1, 0.9 Hz, 2H, ArH), 3.68 (s, 6H, N-CH$_3$). ^{13}C NMR (101 MHz, DMSO-d$_6$) δ 178.98, 157.19, 153.46, 137.99, 137.97, 137.82, 136.63, 129.10, 126.36, 121.69, 121.28, 119.09, 113.22, 110.40, 53.40, 32.89. ESI-MS (m/z): 409.1590 [M$^+$] for $C_{26}H_{20}FN_3O$.

5E: 5′-Fluoro-1*H*,1″*H*-[3,3′:3′,3″-terindol]-2′(1′*H*)-one. Creamy white solid, M. P.: 258–262 °C,[18] ^{1}H NMR (400 MHz, DMSO-d$_6$) δ 10.99 (d, J = 2.3 Hz, 2H, NH), 10.63 (s, 2H, NH), 7.33 (d, J = 0.8 Hz, 1H, ArH), 7.31 (d, J = 0.8 Hz, 1H, ArH), 7.18 (s, 1H, ArH), 7.16 (s, 1H, ArH), 7.06–7.01 (m, 1H, ArH), 7.00–6.98 (m, 3H, ArH), 6.97–6.92 (m, 1H, ArH), 6.85 (d, J = 2.6 Hz, 2H, ArH), 6.78 (ddd, J = 8.0, 7.0, 1.0 Hz, 2H, ArH). ^{13}C NMR (101 MHz, DMSO-d$_6$) δ 179.18, 159.62, 157.26, 138.04, 137.43, 136.82, 126.04, 126.03, 126.02, 124.95, 121.56, 121.11, 118.89, 114.12, 112.22, 53.59. ESI-MS (m/z): 381.1277 [M$^+$] for $C_{24}H_{16}FN_3O$.

5F: 5′-Bromo-1,1″-dimethyl-1*H*,1″*H*-[3,3′:3′,3″-terindol]-2′(1′*H*)-one. Pale white crystalline solid, M. P.: 284–292 °C,[18] ^{1}H NMR (400 MHz, DMSO-d$_6$) δ 10.77 (s, 1H, NH), 7.40–7.37 (m, 2H, ArH), 7.35 (s, 1H, ArH), 7.26 (d, J = 2.0 Hz, 1H, ArH), 7.18 (s, 1H, ArH), 7.16 (s, 1H, ArH), 7.08–7.04 (m, 2H, ArH), 6.92 (d, J = 8.3 Hz, 1H, ArH), 6.89 (s, 2H, ArH), 6.84–6.80 (m, 2H, ArH), 3.68 (s, 6H, N-CH$_3$). ^{13}C NMR (101 MHz, DMSO-d$_6$) δ 178.59, 141.10, 137.84, 137.35, 131.32, 129.04, 127.84, 126.32, 121.74, 121.19, 119.14, 113.80, 113.09, 112.26, 110.47, 53.11, 32.90. ESI-MS (m/z): 469.0790 [M$^+$] for $C_{26}H_{20}BrN_3O$.

5G: 1,1″-Dimethyl-1*H*,1″*H*-[3,3′:3′,3″-terindol]-2′(1′*H*)-one. Snow white powder, M. P.: 282–286 °C,[18] ^{1}H NMR (400 MHz, DMSO-d$_6$) δ 10.61 (s, 1H, NH), 7.35 (s, 1H, ArH), 7.33 (s, 1H, ArH), 7.19 (dd, J = 7.7, 4.8 Hz, 4H, ArH), 7.06–7.02 (m, 2H, ArH), 6.94 (dd, J = 8.2, 0.9 Hz, 1H, ArH), 6.89 (td, J = 7.6, 1.0 Hz, 1H, ArH), 6.84 (s, 2H, ArH), 6.80 (ddd, J = 8.0, 7.1, 0.9 Hz, 1H, ArH), 3.66 (s, 6H, N-CH$_3$). ^{13}C NMR (101 MHz, DMSO-d$_6$) δ 179.08, 141.75, 137.81, 135.00, 128.97, 128.45, 126.51, 125.40, 122.12, 121.52, 118.94, 113.90, 113.88, 110.31, 110.14, 52.88, 32.87. ESI-MS (m/z): 391.1685 [M$^+$] for $C_{26}H_{21}N_3O$.

5H: 1*H*,1″*H*-[3,3′:3′,3″-terindol]-2′(1′*H*)-one. Dull white powder, M. P.: 264–270 °C,[18] ^{1}H NMR (400 MHz, DMSO-d$_6$) δ 10.95 (s, 2H, NH), 10.60 (s, 1H, NH), 7.32 (d, J = 8.1 Hz, 2H, ArH), 7.20 (d, J = 7.7 Hz, 4H, ArH), 6.97 (dd, J = 14.0, 7.3 Hz, 3H, ArH), 6.88 (t, J = 7.5 Hz, 1H, ArH), 6.82 (d, J = 2.4 Hz, 2H, ArH), 6.76 (t, J = 7.5 Hz, 2H, ArH). ^{13}C NMR (101 MHz, DMSO-d$_6$) δ 179.30, 141.84, 137.44, 135.12, 128.38, 126.21, 125.44, 124.81, 122.00, 121.39, 118.76, 114.79, 112.14, 110.10, 53.08. ESI-MS (m/z): 363.1372 [M$^+$] for $C_{24}H_{17}N_3O$.

5I: 5′-Bromo-1*H*,1″*H*-[3,3′:3′,3″-terindol]-2′(1′*H*)-one. Light pink solid, M. P.: 238–242 °C,[18] ^{1}H NMR (400 MHz, DMSO-d$_6$) δ 11.01 (d, J = 2.0 Hz, 2H, NH), 10.76 (s, 1H, NH), 7.39 (dd, J = 8.3, 2.0 Hz, 1H, ArH), 7.33 (d, J = 8.2 Hz, 2H, ArH), 7.26 (d, J =

1.9 Hz, 1H, ArH), 7.16 (d, J = 8.1 Hz, 2H, ArH), 7.00 (dd, J = 11.2, 3.9 Hz, 2H, ArH), 6.93 (d, J = 8.3 Hz, 1H, ArH), 6.85 (d, J = 2.5 Hz, 2H, ArH), 6.79 (t, J = 7.5 Hz, 2H, ArH). ^{13}C NMR (101 MHz, DMSO-d_6) δ 178.78, 141.19, 137.47, 131.23, 127.87, 125.99, 124.96, 121.61, 121.02, 118.96, 113.98, 113.67, 112.25, 53.30. ESI-MS (m/z): 441.0477 [M^+] for $C_{24}H_{16}BrN_3O$.

5J: 6,6″-Dichloro-5′-fluoro-1*H*,1″*H*-[3,3′:3′,3″-terindol]-2′(1′*H*)-one. Cream coloured solid, M. P.: 278–282 °C, ^{1}H NMR (400 MHz, DMSO-d_6) δ 11.15 (d, J = 1.7 Hz, 2H, NH), 10.70 (s, 1H, NH), 7.38 (d, J = 1.7 Hz, 2H, ArH), 7.14 (d, J = 8.6 Hz, 2H, ArH), 7.08–7.00 (m, 2H, ArH), 6.96–6.91 (m, 3H, ArH), 6.82 (dd, J = 8.6, 1.8 Hz, 2H, ArH). ^{13}C NMR (101 MHz, DMSO-d_6) δ 178.81, 159.62, 157.26, 137.98, 137.96, 137.86, 136.19, 136.11, 126.45, 125.98, 124.79, 122.32, 119.40, 114.35, 111.83, 53.23. ESI-MS (m/z): 449.0498 [M^+] for $C_{24}H_{14}Cl_2FN_3O$.

5K: 6,6″-Dichloro-1*H*,1″*H*-[3,3′:3′,3″-terindol]-2′(1′*H*)-one. Orange solid, M. P.: 290–294 °C,[22] ^{1}H NMR (400 MHz, DMSO-d_6) δ 11.11 (d, J = 2.7 Hz, 2H, NH), 10.66 (s, 1H, NH), 7.37 (d, J = 2.3 Hz, 3H, ArH), 7.22–7.13 (m, 3H, ArH), 6.96–6.86 (m, 3H, ArH), 6.80 (dd, J = 8.7, 2.1 Hz, 3H, ArH). ^{13}C NMR (101 MHz, DMSO-d_6) δ 178.90, 141.73, 137.84, 134.49, 128.63, 126.36, 125.80, 125.33, 124.94, 122.45, 122.21, 119.26, 114.99, 111.77, 110.32, 52.71. ESI-MS (m/z): 431.0592 [M^+] for $C_{24}H_{15}Cl_2N_3O$.

5L: 5′-Bromo-6,6″-dichloro-1*H*,1″*H*-[3,3′:3′,3″-terindol]-2′(1′*H*)-one. White solid, M. P.: 268–272 °C, ^{1}H NMR (400 MHz, DMSO-d_6) δ 11.16 (d, J = 2.1 Hz, 2H, NH), 10.82 (s, 1H, NH), 7.41–7.35 (m, 3H, ArH), 7.26 (d, J = 1.9 Hz, 1H, ArH), 7.13 (s, 1H, ArH), 7.11 (s, 1H, ArH), 6.91 (dd, J = 13.1, 5.4 Hz, 3H, ArH), 6.82 (dd, J = 8.6, 1.9 Hz, 2H, ArH). ^{13}C NMR (101 MHz, DMSO-d_6) δ 178.42, 141.09, 137.86, 136.83, 131.51, 127.80, 125.99, 124.73, 122.22, 119.46, 114.19, 114.18, 114.17, 113.89, 112.44, 111.90, 52.92. ESI-MS (m/z): 508.9697 [M^+] for $C_{24}H_{14}$ $BrCl_2N_3O$.

5M: 5-(Bis(1-methyl-1*H*-indol-3-yl)methyl)-4-methylthiazole. Peach coloured solid, M. P.: 238–242 °C, ^{1}H NMR (400 MHz, $CDCl_3$) δ 8.55 (s, 1H, ArH), 7.42 (d, J = 7.9 Hz, 2H, ArH), 7.33 (d, J = 8.2 Hz, 2H, ArH), 7.25 (t, J = 7.5 Hz, 2H, ArH), 7.06 (t, J = 7.4 Hz, 2H, ArH), 6.63 (s, 2H, ArH), 6.11 (s, 1H, CH), 3.70 (s, 6H, N–CH_3), 2.50 (s, 3H, CH_3). ^{13}C NMR (101 MHz, $CDCl_3$) δ 149.87, 148.03, 137.42, 127.81, 127.01, 121.84, 119.78, 119.06, 117.34, 109.43, 32.92, 32.10, 15.44. ESI-MS (m/z): 371.1456 [M^+], found: 371.1428 for $C_{23}H_{21}N_3S$.

5N: 3,3′-(Pyren-1-ylmethylene)bis(1-methyl-1*H*-indole). Wine coloured solid, M. P.: 182–186 °C, ^{1}H NMR (400 MHz, $CDCl_3$) δ 8.47 (d, J = 9.4 Hz, 1H, ArH), 8.18–8.14 (m, 2H, ArH), 8.04–7.97 (m, 5H, ArH), 7.87 (d, J = 8.0 Hz, 1H, ArH), 7.39 (d, J = 7.9 Hz, 2H, ArH), 7.31 (d, J = 8.2 Hz, 2H, ArH), 7.23 (dd, J = 8.1, 0.9 Hz, 2H, ArH), 7.01–6.99 (m, 2H, ArH, 1H, CH), 6.44 (s, 2H, ArH), 3.63 (s, 6H, N-CH_3). ^{13}C NMR (101 MHz, $CDCl_3$) δ 138.29, 137.57, 131.49, 131.00, 130.01, 129.25, 128.75, 127.60, 126.80, 125.89, 125.24, 125.13, 125.02, 124.93, 124.91, 123.93, 121.58, 120.14, 118.80, 118.24, 109.24, 36.18, 32.82. ESI-MS (m/z): 474.2096 [M^+], found: 474.1881 for $C_{35}H_{26}N_2$.

5O: 4-(Bis(1-methyl-1*H*-indol-3-yl)methyl)-2,6-dimethoxyphenol. Light pink powder, M. P.: 166–170 °C,[29] ^{1}H NMR (400 MHz, $CDCl_3$) δ 7.40 (d, J = 7.9 Hz, 2H, ArH), 7.30 (d, J = 8.2 Hz, 2H, ArH), 7.20 (t, J = 7.5 Hz, 2H, ArH), 7.00 (t, J = 7.4 Hz, 2H, ArH), 6.59 (s, 2H, ArH), 6.53 (s, 2H, ArH), 5.80 (s, 1H, OH), 5.43 (s, 1H, CH), 3.76 (s, 6H, OCH_3), 3.69 (s, 6H, N-CH_3). ^{13}C NMR (101 MHz, $CDCl_3$) δ 146.88, 137.48, 135.84, 132.87, 128.35, 127.50, 121.50, 120.16, 118.71, 118.36, 109.16, 105.46, 56.36, 40.38, 32.83. ESI-MS (m/z): 426.1943 [M^+] for $C_{27}H_{26}N_2O_3$.

5P: 4-(Bis(6-fluoro-1*H*-indol-3-yl)methyl)-*N*,*N*-dimethylaniline. Wine colour solid, M. P.: 152–156 °C, ^{1}H NMR (400 MHz, $CDCl_3$) δ 7.92 (s, 2H, NH), 7.28 (s, 1H, ArH), 7.25 (s, 1H, ArH), 7.16 (d, J = 7.3 Hz, 2H, ArH), 7.00 (d, J = 9.6 Hz, 2H, ArH), 6.74–6.68 (m, 4H, ArH), 6.60 (s, 2H, ArH), 5.70 (s, 1H, CH), 2.91 (s, 6H, N-CH_3). ^{13}C NMR (101 MHz, $CDCl_3$) δ 161.11, 158.75, 136.62, 129.26, 123.77, 123.74, 120.75, 120.31, 112.89, 108.10, 107.85, 97.50, 97.25, 41.00, 39.21. ESI-MS (m/z): 401.1704 [M^+] for $C_{25}H_{21}F_2N_3$.

5Q: 3,3′-(1-(3,4-Dimethoxyphenyl)ethane-1,1-diyl)bis(1-methyl-1*H*-indole). Creamy yellow solid, M. P.: 134–138 °C, ^{1}H NMR (400 MHz, $CDCl_3$) δ 7.34 (dd, J = 8.0, 0.8 Hz, 2H, ArH), 7.29 (d, J = 8.2 Hz, 2H, ArH), 7.17 (ddd, J = 8.2, 7.0, 1.0 Hz, 2H, ArH), 7.01 (d, J = 2.2 Hz, 1H, ArH), 6.96–6.89 (m, 3H, ArH), 6.75 (d, J = 8.5 Hz, 1H, ArH), 6.49 (s, 2H, ArH), 3.86 (s, 3H, OCH_3), 3.67 (d, J = 2.6 Hz, 3H, OCH_3; 6H, N-CH_3), 2.34 (s, 3H, CH_3). ^{13}C NMR (101 MHz, $CDCl_3$) δ 148.12, 146.95, 141.30, 137.85, 128.15, 126.88, 123.56, 122.32, 121.12, 120.41, 118.44, 111.98, 110.36, 109.24, 55.85, 43.46, 32.75, 29.39. ESI-MS (m/z): 424.2151 [M^+], found: 424.2140 for $C_{28}H_{28}N_2O_2$.

5R: 3,3′-(1-(*p*-Tolyl)ethane-1,1-diyl)bis(1-methyl-1*H*-indole). Beige coloured powder, M. P.: 170–174 °C,[30] ^{1}H NMR (400 MHz, $CDCl_3$) δ 7.33 (d, J = 8.0 Hz, 2H, ArH), 7.29 (dd, J = 8.3, 2.2 Hz, 4H, ArH), 7.17 (ddd, J = 8.2, 7.0, 1.0 Hz, 2H, ArH), 7.06 (d, J = 8.0 Hz, 2H, ArH), 6.94 (ddd, J = 8.0, 7.0, 1.0 Hz, 2H, ArH), 6.50 (s, 2H, ArH), 3.67 (s, 6H, N-CH_3), 2.34 (d, J = 5.7 Hz, 6H, CH_3). ^{13}C NMR (101 MHz, $CDCl_3$) δ 145.46, 137.85, 135.10, 128.57, 127.09, 126.94, 123.55, 122.33, 121.07, 118.39, 109.22, 43.41, 32.73, 29.28, 21.11. ESI-MS (m/z): 378.2096 [M^+] for $C_{27}H_{26}N_2$.

5S: 3,3′-(Cyclopentane-1,1-diyl)bis(1-methyl-1*H*-indole). Dark pink powder, M. P.: 114–118 °C, ^{1}H NMR (400 MHz, $CDCl_3$) δ 7.54 (d, J = 8.0 Hz, 2H, ArH), 7.25 (s, 1H, ArH), 7.23 (s, 1H, ArH), 7.15–7.11 (m, 2H, ArH), 6.95–6.91 (m, 4H, ArH), 3.73 (s, 6H, N-CH_3), 2.52 (s, 4H, CH_2), 1.84 (s, 4H, CH_2). ^{13}C NMR (101 MHz, $CDCl_3$) δ 137.93, 126.95, 126.14, 122.11, 121.43, 120.97, 118.06, 109.16, 46.18, 39.05, 32.79, 24.18. ESI-MS (m/z): 328.1939 [M^+], found: 327.5009 for $C_{23}H_{24}N_2$.

5T: 3,3′-(Cyclohexane-1,1-diyl)bis(1-methyl-1*H*-indole). Moss coloured solid, M. P.: 166–170 °C[31], ^{1}H NMR (400 MHz, $CDCl_3$) δ 7.63 (d, J = 8.4 Hz, 3H, ArH), 7.26 (d, J = 11.3 Hz, 2H, ArH), 7.14 (t, J = 8.3 Hz, 1H, ArH), 6.97–6.92 (m, 4H, ArH), 3.74 (s, 6H, N-CH_3), 2.59–2.56 (m, 4H, CH_2), 1.72–1.59 (m, 6H, CH_2). ^{13}C NMR (101 MHz, $CDCl_3$) δ 137.78, 127.15, 126.80, 122.33, 121.76, 120.83, 118.04, 109.23, 39.77, 37.20, 32.83, 26.91, 23.17. ESI-MS (m/z): 342.2096 [M^+] for $C_{24}H_{26}N_2$.

5U: 3,3-Dimethyl-5,5-bis(1-methyl-1*H*-indol-3-yl)cyclohexan-1-one. Dark purple solid, M. P.: 98–102 °C, ^{1}H NMR (400 MHz, $CDCl_3$) δ 8.00 (d, J = 7.4 Hz, 2H, ArH), 7.34 (dd, J = 25.0, 18.5 Hz, 6H, ArH), 6.67 (s, 2H, ArH), 3.81 (s, 6H, N-CH_3), 2.66 (s, 3H, CH_2), 2.34 (s, 3H, CH_2), 1.13 (s, 6H, CH_3).^{13}C NMR (101 MHz, $CDCl_3$) δ 200.09, 153.05, 138.21, 130.83, 125.59, 123.04, 121.50, 120.36, 115.05, 110.12, 51.04, 42.72, 33.48, 33.40, 33.25, 28.64. ESI-MS (m/z): 384.2202 [M^+], found: 385.2278 for $C_{26}H_{28}N_2O$.

Conclusion

The biochar-modified g-$C_3N_4 \cdot SO_3H$ (BCNSA) catalyst represents a significant advancement in bis-indole synthesis, facilitating efficient reactions between indoles and carbonyl-group containing reactants under sustainable conditions. Characterized by SEM, EDX, mapping, TGA, IR, and XRD, the catalyst exhibits structural integrity and functionality. XRD analysis revealed key changes *i.e.* the disappearance of the 13.12° peak, a shift in the peak from 27.84° to 25.44°, and a new peak at 42.79°, indicating disrupted g-C_3N_4 order, altered interlayer spacing, and a new crystalline phase from SO_3H incorporation. FE-SEM images showed a graphite-like structure with distinct layers and a porous morphology. EDX spectra and elemental mapping confirmed the uniform dispersion of C, N, S, and O from functionalized sulfonic acid groups, indicating successful modification, and TGA showed only 19% loss up to 500 °C and a total loss of 42.6% mass at 1000 °C, confirming its high thermal stability. The catalyst achieved impressive yields of 80–98% in 5–45 minutes for a variety of bis-indoles, demonstrating successful gram-scale synthesis and reusability over six cycles. Green chemistry metrics highlight its efficiency, with a low *E*-factor (0.064–0.30), high atom economy (94.78–96.30%), excellent reaction mass efficiency (76.41–93.97%), and a superior process mass intensity (1.07–1.32). An eco-score of 70–79.24 underscores its minimal environmental impact. Therefore, it may be concluded that BCNSA's unique properties may open avenues for new organic transformations in the scientific community, with further research potentially uncovering even more efficient and environmentally friendly synthetic methods.

Data availability

All data generated and analyzed during this study, including ^{1}H and ^{13}C NMR spectra of the synthesized compounds, are provided in the ESI† file.

Conflicts of interest

The authors confirmed that this article has no conflict of interest.

Acknowledgements

The authors express their gratitude to the Department of Chemistry, MLSU, Udaipur, for providing research facilities, as well as to PDEU, Gandhinagar, SAIF-IIT Madras, and IIT Bombay for conducting the XRD, HRSEM, and TGA/DTA analyses, respectively. S. Agarwal and S. Teli acknowledge the financial support from DST-SERB, SURE (No. SUR/2022/001312). S. Agarwal also sincerely thanks the Ministry of Education, SPD-RUSA Rajasthan, for the NMR facility provided under the RUSA 2.0 Research and Innovation project (File No. RUSA/GEN/MLSU/2020/6394).

References

1 S. Soni, N. Sahiba, S. Teli, P. Teli, L. K. Agarwal and S. Agarwal, Advances in the synthetic strategies of benzoxazoles using 2-aminophenol as a precursor: an up-to-date review, *RSC Adv.*, 2023, **13**(34), 24093–24111.
2 P. Teli, S. Soni, S. Teli and S. Agarwal, Unlocking diversity: from simple to cutting-edge synthetic methodologies of bis(indolyl) methanes, *Top. Curr. Chem.*, 2024, **382**(1), 8.
3 B. Prabagar, Y. Yang and Z. Shi, Site-selective C–H functionalization to access the arene backbone of indoles and quinolines, *Chem. Soc. Rev.*, 2021, **50**(20), 11249–11269.
4 S. Nasri, M. Bayat, F. R. Miankooshki and N. H. Samet, Recent developments in green approaches for sustainable synthesis of indole-derived scaffolds, *Mol. Diversity*, 2022, 1–35.
5 S. Imran, M. Taha and N. Hadiani Ismail, A review of bisindolylmethane as an important scaffold for drug discovery, *Curr. Med. Chem.*, 2015, **22**(38), 4412–4433.
6 V. D. Kadu, S. N. Chandrudu, M. G. Hublikar, D. G. Raut and R. B. Bhosale, Metal-free oxidative coupling of arylmethylamines with indoles: a simple, environmentally benign approach for the synthesis of 3,3′-bis(indolyl) methanes, *RSC Adv.*, 2020, **10**(39), 23254–23262.
7 G. B. Pund, D. B. Wahul, T. R. Deshmukh, S. T. Dhumal, K. R. Mandave, S. A. Gaware, M. Farooqui, B. S. Dobhal and M. J. Hebade, Theophylline hydrogen sulfate: a green and efficient catalyst for synthesis of 3,3-bis(1*H*-indol-3-yl) indolin-2-one derivatives, *Synth. Commun.*, 2023, **53**(13), 1008–1019.
8 M. E. Adly, A. M. Mahmoud and H. B. El-Nassan, Green electrosynthesis of bis(indolyl) methane derivatives in deep eutectic solvents, *BMC Chem.*, 2024, **18**(1), 139.
9 K. A. Chavan, M. Shukla, A. N. S. Chauhan, S. Maji, G. Mali, S. Bhattacharyya and R. D. Erande, Effective synthesis and biological evaluation of natural and designed bis(indolyl) methanes *via* taurine-catalyzed green approach, *ACS Omega*, 2022, **7**(12), 10438–10446.
10 R. A. Sheldon, Engineering a more sustainable world through catalysis and green chemistry, *J. R. Soc. Interface*, 2016, **13**(116), 20160087.
11 E. A. Mohamed, M. A. Betiha and N. A. Negm, Insight into the recent advances in sustainable biodiesel production by catalytic conversion of vegetable oils: current trends, challenges, and prospects, *Energy Fuels*, 2023, **37**(4), 2631–2647.
12 S. Soni, S. Teli, P. Teli and S. Agarwal, Empowering sustainability: charting the seven years of progress in g-C_3N_4 based materials and their crucial role in building a greener future, *Sustainable Chem. Pharm.*, 2024, **41**, 101693.
13 L. Liang, F. Xi, W. Tan, X. Meng, B. Hu and X. Wang, Review of organic and inorganic pollutants removal by biochar and biochar-based composites, *Biochar*, 2021, **3**, 255–281.
14 S. Teli, S. Soni, P. Teli, N. Sahiba and S. Agarwal, Unlocking the potential of *Ficus religiosa* tree bark-derived biochar sulfonic acid: a journey from synthesis and

characterization to its astonishing catalytic role in green synthesis of perimidines, *Res. Chem. Intermed.*, 2024, **50**(3), 1475–1495.

15 S. Soni, P. Teli, N. Sahiba, S. Teli and S. Agarwal, Exploring the synthetic potential of a g-C_3N_4·SO_3H ionic liquid catalyst for one-pot synthesis of 1,1-dihomoarylmethane scaffolds *via* Knoevenagel–Michael reaction, *RSC Adv.*, 2023, **13**(19), 13337–13353.

16 H. Venkatesvaran, S. Balu, A. Chowdhury, S.-W. Chen and T. C.-K. Yang, Photo–Redox Properties of SO_3H Functionalized Metal-Free g-C_3N_4 and Its Application in the Photooxidation of Sunset Yellow FCF and Photoreduction of Cr(VI), *Catalysts*, 2022, **12**(7), 751.

17 H. Veisi, P. Mohammadi and T. Ozturk, Design, synthesis, characterization, and catalytic properties of g-C_3N_4-SO_3H as an efficient nanosheet ionic liquid for one-pot synthesis of pyrazolo[3,4-*b*] pyridines and bis(indolyl) methanes, *J. Mol. Liq.*, 2020, **303**, 112625.

18 G. Brahmachari and B. Banerjee, Facile and one-pot access of 3,3-bis(indol-3-yl) indolin-2-ones and 2,2-bis(indol-3-yl) acenaphthylen-1(2*H*)-one derivatives *via* an eco-friendly pseudo-multicomponent reaction at room temperature using sulfamic acid as an organo-catalyst, *ACS Sustain. Chem. Eng.*, 2014, **2**(12), 2802–2812.

19 P. Paira, A. Hazra, S. Kumar, R. Paira, K. B. Sahu, S. Naskar, S. Mondal, A. Maity, S. Banerjee and N. B. Mondal, Efficient synthesis of 3,3-diheteroaromatic oxindole analogues and their *in vitro* evaluation for spermicidal potential, *Bioorg. Med. Chem. Lett.*, 2009, **19**(16), 4786–4789.

20 J. Azizian, A. A. Mohammadi, N. Karimi, M. R. Mohammadizadeh and A. R. Karimi, Silica sulfuric acid a novel and heterogeneous catalyst for the synthesis of some new oxindole derivatives, *Catal. Commun.*, 2006, **7**(10), 752–755.

21 S. Mathavan, K. Kannan and R. B. Yamajala, Thiamine hydrochloride as a recyclable organocatalyst for the synthesis of bis(indolyl)methanes, tris(indolyl)methanes, 3,3-di (indol-3-yl)indolin-2-ones and biscoumarins, *Org. Biomol. Chem.*, 2019, **17**(44), 9620–9626.

22 W. Huang, L. Nang, X. Li, L. Yuan, Y. Ma and D. Liang, Bromine/*para*-Toluenesulfonic Acid-Catalyzed Synthesis of 3,3-Bis(indole-3-yl)indoline-2-(1*H*)-ones by Condensing Indoles with Isatins, *Chin. J. Chem.*, 2015, **33**(10), 1167–1172.

23 Y. A. Tayade, D. R. Patil, Y. B. Wagh, A. D. Jangle and D. S. Dalal, An efficient synthesis of 3-indolyl-3-hydroxy oxindoles and 3,3-di(indolyl) indolin-2-ones catalyzed by sulfonated β-CD as a supramolecular catalyst in water, *Tetrahedron Lett.*, 2015, **56**(5), 666–673.

24 Y. Sarrafi, K. Alimohammadi, M. Sadatshahabi and N. Norozipoor, An improved catalytic method for the synthesis of 3,3-di(indolyl) oxindoles using Amberlyst 15 as a heterogeneous and reusable catalyst in water, *Monatsh. Chem.*, 2012, **143**, 1519–1522.

25 W. E. Noland, H. V. Kumar, G. C. Flick, C. L. Aspros, J. H. Yoon, A. C. Wilt, N. Dehkordi, S. Thao, A. K. Schneerer and S. Gao, Hydrated ferric sulfate-catalyzed reactions of indole with aldehydes, ketones, cyclic ketones, and chromanones: synthesis of bisindoles and trisindoles, *Tetrahedron*, 2017, **73**(27–28), 3913–3922.

26 P. Teli, N. Sahiba, A. Sethiya, J. Soni and S. Agarwal, Triethylammonium hydrogen sulfate ionic liquid-assisted highly efficient synthesis of bis(indoyl) methanes, *Polycyclic Aromat. Compd.*, 2024, **44**(2), 883–896.

27 P. M. Nowak, R. Wietecha-Posłuszny and J. Pawliszyn, White analytical chemistry: an approach to reconcile the principles of green analytical chemistry and functionality, *Trac. Trends Anal. Chem.*, 2021, **138**, 116223.

28 S. Soni, S. Teli, P. Teli, A. Manhas, P. C. Jha and S. Agarwal, Highly efficient synthesis of isoxazolones and pyrazolones using g-C_3N_4·OH nanocomposite with their *in silico* molecular docking, pharmacokinetics and simulation studies, *Sci. Rep.*, 2024, **14**(1), 19123.

29 D. Konwar and U. Bora, Free Radical Triggered Convenient Synthesis of Bis(indolyl) methane with Potassium Peroxodisulfate as Catalyst, *ChemistrySelect*, 2020, **5**(25), 7460–7466.

30 C. Ferrer, C. H. Amijs and A. M. Echavarren, Intra-and Intermolecular Reactions of Indoles with Alkynes Catalyzed by Gold, *Chem.–Eur. J.*, 2007, **13**(5), 1358–1373.

31 S. D. Pasuparthy, P. Somkuwar, V. Kali, A. K. S. Kalleshappa and B. Maiti, Synthesis of dimeric indoles from Friedel–Crafts reaction of indoles with ketones catalysed by a Brønsted acid ionic liquid and their interactions with BSA and DNA, *New J. Chem.*, 2024, **48**(34), 14904–14923.